


Incomplete spontaneous decay in a waveguide caused by polarization selection

A. S. Kuraptsev^{*} and I. M. Sokolov[†]

Peter the Great St. Petersburg Polytechnic University, 195251 St. Petersburg, Russia

 (Received 8 July 2019; revised manuscript received 14 October 2019; accepted 1 May 2020; published 22 May 2020)

Spontaneous decay of an excited atom in a waveguide is essentially modified by the spatial structure of a vacuum reservoir. This is particularly exciting in view of a range of applications for quantum information science. We found out that spontaneous decay can be incomplete, so the time dependence of the excited state population asymptotically approaches to a nonzero value, under the conditions when the atomic transition frequency is larger than the cutoff frequency of a waveguide and far from the vicinities of the cutoffs. The discovered effect is explained by the emergence of the dark state, which is nondecaying due to polarization selection rules. It was revealed for a single-mode waveguide with rectangular cross section both in a single-atom case and a diatomic case when the long-range dipole-dipole interaction plays a significant role.

DOI: [10.1103/PhysRevA.101.053852](https://doi.org/10.1103/PhysRevA.101.053852)

I. INTRODUCTION

Atomic spontaneous decay is one of the most fundamental phenomena of quantum electrodynamics, taking place due to the coupling between an atom and vacuum reservoir. Now it is well understood that changing the properties of the reservoir can affect the spontaneous decay process. Thus, placing an atom in a cavity or waveguide leads to significant alteration of the decay rate [1–8]. In the case of a waveguide, this effect dramatically depends on the ratio between the resonant frequency of atomic transition ω_0 and the cutoff frequency of a waveguide ω^c . In particular, in the well-known paper of Kleppner [3], strong suppression of spontaneous decay under condition $\omega_0 < \omega^c$ was predicted. The same effect takes place for an excited atom in photonic band gap crystals when ω_0 falls in the range of the frequency gap of the environment [9,10]. When ω_0 approaches the vicinities of a photonic crystal band gap where the local density of states is not smooth, the suppression of decay is not complete, but only partial, so only some part of the energy of the initial atomic excitation is transferred to the electromagnetic field and the other part remains in the atomic system. This effect is explained by frequency selection and can be described in the framework of two-level atom formalism neglecting the vectorial nature of electromagnetic waves, as was done in Ref. [10].

In this paper we report the incomplete spontaneous decay in a waveguide when the atomic transition frequency ω_0 is larger than ω^c and far from the vicinities of the cutoffs of the waveguide modes. We explain the revealed effect by polarization selection. Our results raise the issue of the role that polarization plays in the problem of spontaneous decay in structured reservoirs. The revealed effect might be of general interest in different topics of quantum physics; in particular, quantum information storing and processing [11,12]. It can be useful for the development and improvement of many

quantum devices based on atomic systems in a waveguide, such as single-photon switching [13–15], routers [16], transistors [17–19], frequency comb generators [20], and single-photon frequency converters [21].

II. BASIC ASSUMPTIONS AND APPROACH

The theory employed here considers an ensemble of point-like motionless atoms in a waveguide. This model is excellent for ensembles of impurity atoms embedded in a transparent dielectric under low temperatures that, therefore, provide a fantastic and practically realizable playground for testing the theory [22,23]. For concreteness, we assume that the atoms are equal, having a nondegenerate ground state $|g_i\rangle$ with energy E_g and the total angular momentum $J_g = 0$ and an excited state $|e_i\rangle$ with $E_e = E_g + \hbar\omega_0$, $J_e = 1$ and natural free space linewidth γ_0 (\hbar is the Planck's constant and the index $i = 1, \dots, N$ denotes quantities corresponding to the atom i among N atoms). The excited state is thus triply degenerate and splits into three Zeeman sublevels $|e_{i,m_j}\rangle$, which differ by the angular momentum projection on the quantization axis $z - m_j = -1, 0, 1$. For convenience, let us choose the z axis coinciding with the axis of a waveguide. Assuming the walls of a waveguide to be perfectly conductive (i.e., neglecting the absorption), we can write the non-steady-state Schrödinger equation for the wave function of the joint system, which consists of the atoms and the electromagnetic field in a waveguide, including a vacuum reservoir. This system is described by the following Hamiltonian [24]:

$$\begin{aligned} \hat{H} = & \sum_{i=1}^N \sum_{m_j=-1}^1 \hbar\omega_0 |e_{i,m_j}\rangle \langle e_{i,m_j}| \\ & + \sum_{\mathbf{k}, \alpha} \hbar\omega_k \left(\hat{a}_{\mathbf{k}, \alpha}^\dagger \hat{a}_{\mathbf{k}, \alpha} + \frac{1}{2} \right) - \sum_{i=1}^N \hat{\mathbf{d}}_i \cdot \hat{\mathbf{E}}(\mathbf{r}_i) \\ & + \frac{1}{2\epsilon_0} \sum_{i \neq j}^N \hat{\mathbf{d}}_i \cdot \hat{\mathbf{d}}_j \delta(\mathbf{r}_i - \mathbf{r}_j), \end{aligned} \quad (1)$$

^{*}aleksej-kurapcev@yandex.ru

[†]ims@is12093.spb.edu

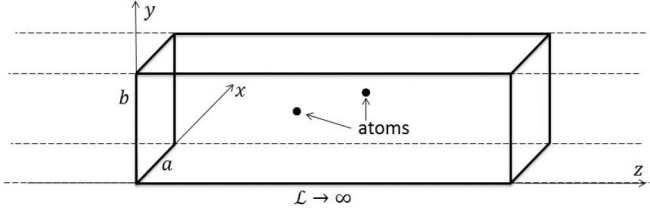


FIG. 1. Sketch of the waveguide and the atoms inside it.

where the first two terms correspond to noninteracting atoms and the electromagnetic field in an empty waveguide, respectively; the third term describes the interaction between the atoms and the field in the dipole approximation; and the last, the contact term, ensures the correct description of the electromagnetic field radiated by the atoms [24]. In Eq. (1), $\hat{a}_{\mathbf{k},\alpha}^\dagger$ and $\hat{a}_{\mathbf{k},\alpha}$ are the operators of creation and annihilation of a photon in the corresponding mode, ω_k is the photon frequency, $\hat{\mathbf{d}}_i$ is the dipole operator of the atom i , $\hat{\mathbf{E}}(\mathbf{r})$ is the electric displacement vector in a waveguide, and \mathbf{r}_i is the position of the atom i .

Field operator $\hat{\mathbf{E}}(\mathbf{r})$ can be obtained on the basis of well-known classical mode expansion of the electromagnetic field in a waveguide [25] followed by standard quantization [26]. The specific form of this operator is determined by the cross section of a waveguide. For concreteness, we assume the rectangular cross section with sizes a and b . In this case, $\hat{\mathbf{E}}(\mathbf{r})$ is given as follows:

$$\hat{\mathbf{E}}(\mathbf{r}) = \sum_{\mathbf{k},\alpha} \sqrt{\frac{\hbar}{2\omega_k}} \mathbf{E}_{\mathbf{k},\alpha}(x,y) \exp(ik_z z) \hat{a}_{\mathbf{k},\alpha} + \text{H.c.}, \quad (2)$$

where α denotes the type of waveguide mode—TE (transverse electric) or TM (transverse magnetic), i means imaginary unit.

$$E_{\mathbf{k},\text{TE}}^x(x,y) = -\frac{ik_n k}{k_m^2 + k_n^2} B_{mn} \cos(k_m x) \sin(k_n y), \quad (3)$$

$$E_{\mathbf{k},\text{TE}}^y(x,y) = \frac{ik_m k}{k_m^2 + k_n^2} B_{mn} \sin(k_m x) \cos(k_n y), \quad (4)$$

$$E_{\mathbf{k},\text{TE}}^z(x,y) \equiv 0, \quad (5)$$

$$E_{\mathbf{k},\text{TM}}^x(x,y) = \frac{ik_z k_m}{k_m^2 + k_n^2} B_{mn} \cos(k_m x) \sin(k_n y), \quad (6)$$

$$E_{\mathbf{k},\text{TM}}^y(x,y) = \frac{ik_z k_n}{k_m^2 + k_n^2} B_{mn} \sin(k_m x) \cos(k_n y), \quad (7)$$

$$E_{\mathbf{k},\text{TM}}^z(x,y) = B_{mn} \sin(k_m x) \sin(k_n y). \quad (8)$$

Here $k_m = m\pi/a$, $k_n = n\pi/b$, and $k = \sqrt{k_m^2 + k_n^2 + k_z^2} = \omega_k/c$. The indexes m and n are positive integers for TM modes, and for TE modes $m, n = 0, 1, 2, \dots$, herewith both indexes cannot be zero together. B_{mn} is the normalization constant, which can be obtained on the basis of the standard form of the field Hamiltonian. A reference point is chosen at one of the corners of the cross section, so the space into a waveguide corresponds to the positive values of the coordinates x and y (see Fig. 1).

Formally solving the Schrödinger equation for the system “atoms+field” and restricting ourselves by the states containing no more than one photon (i.e., neglecting nonlinear

effects), one obtains a system of equations for the amplitudes b_e of onefold atomic excited states with the coupling between atoms described by the so-called Green’s matrix [27]. It is essentially built up of Green’s functions of Maxwell equations, describing the propagation of light in a waveguide from one atom to another. This $3N \times 3N$ matrix plays a key role in the theory, describing both single-atom effects and the radiative transfer between different atoms.

According to the general quantum microscopic approach essentially based on the coupled-dipole model, the Green’s matrix $G_{ee'}(\omega)$ is given as follows:

$$G_{ee'}(\omega) = -\frac{2}{\gamma_0} \left\{ \sum_g V_{e;g} V_{g;e'} \zeta(\hbar\omega - E_g) + \sum_{ee'} V_{e;ee'} V_{ee';e'} \zeta(\hbar\omega - E_{ee'}) \right\}. \quad (9)$$

This equation includes matrix elements of the operator \hat{V} of the interaction between atoms and electromagnetic field; $\zeta(x)$ is a singular function which is determined by the relation $\zeta(x) = \lim_{k \rightarrow \infty} [1 - \exp(ikx)]/x$. To calculate the Green’s matrix, we should perform a summation over resonant single-photon states “ g ” as well as over nonresonant states with two excited atoms and one photon “ ee ” (as greater length, see [27]). Actually, this approach allows one to describe from a single position both monatomic dynamics and cooperative effects caused by interatomic dipole-dipole interaction. The main idea of this approach was first proposed by Foldy [28]; further, it was developed by a number of authors; [29–33], to name a few. This method was successfully used in our group for the analysis of the optical properties of dense atomic ensembles as well as for studying light scattering from such ensembles [34–40]. Further, it allowed us to describe cooperative effects in atomic ensembles located in a Fabry-Perot cavity [41,42] and near a conducting surface [43–45]. The calculation of the explicit expressions for the Green’s matrix corresponding to a waveguide is provided in the Appendix.

III. RESULTS AND DISCUSSION

A. Single-atom effect

We first analyze the spontaneous decay dynamics of a single excited atom placed in a waveguide. The character of decay dramatically depends on the transverse sizes of a waveguide a and b , because these sizes determine the cutoff frequency. Without any restriction of generality, we assume $a \geq b$. It is known that if the resonant frequency of atomic transition ω_0 is less than the cutoff frequency of a waveguide ω^c , then single-atom spontaneous decay is totally suppressed for any Zeeman sublevel [3]. This is explained by the fact that in such a case, no one field mode at the transition frequency can propagate in a waveguide as oscillating wave. Different modes have different cutoff frequencies, and ω^c is determined by the mode, which has a minimal one. In the considered case, it is a TE₁₀ mode, so $\omega^c = \omega_{10}^c = c\pi/a$. When $\omega_0 > \omega_{10}^c$, single-atom spontaneous decay is allowed, but the character of this decay depends on the Zeeman sublevel which was initially populated. The developed theory allows us to consider an arbitrary initial condition. From the experimental point of

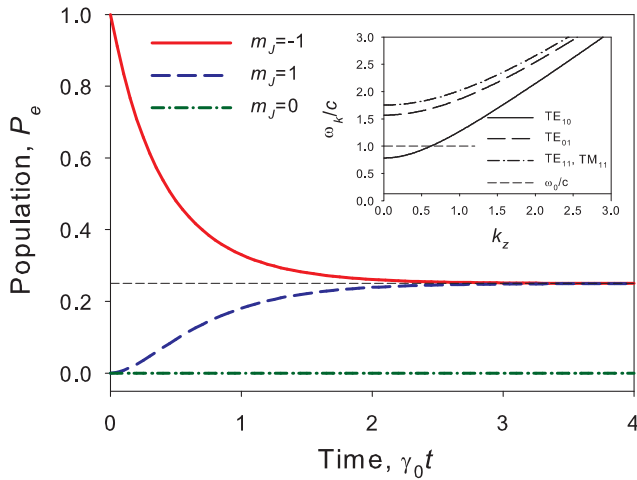


FIG. 2. Population of different Zeeman sublevels of the atomic excited state depending on time. The transverse sizes of a waveguide $a = 4, b = 2$. An atom is located at the axis of a waveguide. At $t = 0$ only one sublevel $m_J = -1$ is populated.

view, this is determined by the technique employed to excite atoms. Generally, an atom can be prepared in a superposition of the ground state and all the Zeeman sublevels of the excited state. For clarity, we first consider the case when at initial time only one Zeeman sublevel $m_J = -1$ is populated with 100% probability. Electromagnetic field is initially in the vacuum state.

Figure 2 shows the population dynamics of all Zeeman sublevels of the atomic excited state $P_e(t) = |b_e(t)|^2$ calculated for a given initial condition. The transverse sizes of a waveguide were chosen as $a = 4, b = 2$ (hereafter we consider the inverse wave number of radiation resonant to the atomic transition $k_0^{-1} = c/\omega_0$ as a unit of length). In this case, the transition frequency ω_0 significantly exceeds the cutoff frequency of a waveguide, $\omega_0/\omega^c = 4/\pi \approx 1.27$, and it is far from the vicinities of the cutoffs of all the waveguide modes (under the considered assumption of perfectly conducting walls of a waveguide, these vicinities are infinitely narrow). The waveguide with given transverse sizes is single mode, because the cutoff frequencies of all the modes except TE_{10} exceed ω_0 (see the inset in Fig. 2). Thus, only the TE_{10} mode is responsible for the spontaneous decay. An atom was considered at the axis of a waveguide. In Fig. 2 we see that the excitation probability of the sublevel $m_J = -1$ decreases with time from its initial value equal to 1 and asymptotically approaches to 0.25 at large times. Thus, we observe incomplete spontaneous decay. It is obvious that the well-known mechanism of decay suppression which was described in Refs. [3] and [10], namely, frequency selection, cannot explain the observed effect under considered conditions. Moreover, we see the gradual population of another Zeeman sublevel— $m_J = 1$. Its excitation probability grows from the initial value equal to 0, and approaches at large times to the same asymptotic value 0.25. The sublevel $m_J = 0$ of the excited state does not populate with time.

To explain the nature of the dependencies plotted in Fig. 2, let us take into account that the process of spontaneous decay is caused by the multiple emission and subsequent absorption

of virtual photons. The vector of electric field in the mode TE_{10} has only one nonzero component along the y axis that is clear from Eqs. (3)–(5). Therefore, upon the atomic transition from the sublevel $m_J = -1$ to the ground state, only half of the energy of atomic excitation transfers to the field subsystem with the y -polarized photon. The subsequent absorption of the y -polarized virtual photon leads to an equiprobable excitation of the sublevels $m_J = -1$ and $m_J = 1$. Thus, as a result of the multiple emission and absorption, a half of the energy of atomic excitation transfers to the electromagnetic field, and the remaining half is equally distributed among the sublevels $m_J = -1$ and $m_J = 1$. The sublevel $m_J = 0$ does not populate because the electric field in TE_{10} has no z component. We call the described mechanism a “polarization selection.” In the considered example, the dipole momentum of the transition from the excited state $m_J = -1$ to the ground state has only one circular component σ^- , which can be presented as a superposition of two linear components x and y . The y component is decaying, while the decay of the x component is forbidden because the TE_{10} mode has no corresponding component of the electric field. In fact, the effect of polarization selection occurs upon the decay of such a superposition state, in which some components are decaying while others correspond to the dark state, which is nondecaying due to polarization effects.

Note that the effects described here can be correctly explained and clearly understood only if the polarization properties are taken into account. In the literature, one can find different approaches to the description of the dynamics of a two-level system (atom) embedded into a waveguide. In a number of them, one-dimensional approximation for the photon mode involved in the interaction is used (see, e.g., Ref. [46]). In general, the description of polarization effects requires a realistic three-dimensional model for the photon modes. This allows us to describe correctly the atomic dynamics both in a single-mode and in a multimode waveguide.

Since the Green’s matrix is only 3×3 in the case of a single atom, we are able to obtain the analytical expressions for the quantum amplitudes of the onefold atomic excited states $b_e(t)$ and, consequently, $P_e(t)$. For the sublevel $m_J = -1$:

$$b_e(t) = \frac{i}{2} \left[1 + \exp\left(-\frac{\gamma'}{2}t\right) \right],$$

$$P_e(t) = \frac{1}{4} \left[1 + 2 \exp\left(-\frac{\gamma'}{2}t\right) + \exp(-\gamma't) \right].$$

Thus, the spontaneous decay dynamics is described by biexponential law. For the considered parameters $\gamma' \approx 3.8\gamma_0$.

For Zeeman sublevel $m_J = 1$ the dynamics is described as follows:

$$b_e(t) = \frac{i}{2} \left[-1 + \exp\left(-\frac{\gamma'}{2}t\right) \right],$$

$$P_e(t) = \frac{1}{4} \left[1 - 2 \exp\left(-\frac{\gamma'}{2}t\right) + \exp(-\gamma't) \right].$$

Note that the curves shown in Fig. 2 were obtained upon a specific initial condition—when only one sublevel $m_J = -1$ was excited at $t = 0$. Of course, upon another initial condition the results will differ. Thus, if the sublevel $m_J = 0$ of the

excited state is initially populated, then spontaneous decay is totally suppressed, i.e., $P_e(t) \equiv 1$ for $m_J = 0$ and $P_e(t) \equiv 0$ for $m_J = \pm 1$. This is explained by the fact that the spontaneous decay of a given sublevel requires the presence of field modes with a nonzero z component that can propagate in a waveguide as an oscillating wave. In the case when the sublevel $m_J = 1$ is initially populated, the results are mirror symmetrical to those shown in Fig. 1 (i.e., the curves for $m_J = -1$ and $m_J = 1$ are swapped).

The rate of incomplete spontaneous decay is determined by the parameter γ' . It depends on the position of the atom in the plane perpendicular to the axis of a waveguide (there is no dependence on its z position, because all the points along the z axis are physically equal in an infinite waveguide). By the analysis of the eigenvalues of the Green's matrix, we derived the expression for γ' :

$$\gamma' = \frac{6\pi\gamma_0}{k_0^2 ab \sqrt{1 - \left(\frac{\pi}{k_0 a}\right)^2}} \sin^2\left(\frac{\pi x_1}{a}\right), \quad (10)$$

where x_1 means the x coordinate of the atom. Note that γ' does not depend on its y coordinate. The reason for this feature is that the electric field in the TE₁₀ mode has no dependence on y , which is clear from Eq. (4).

To verify the explanation of the observed effect, we changed the frequency of atomic transition. The alteration in ω_0 , if it does not cross the cut-offs of the waveguide modes, cannot qualitatively change the picture.

We carried out the calculations of the atomic excitation dynamics in a waveguide with different transverse sizes. Our analysis shows that in the case of a multimode waveguide, the effect of incomplete spontaneous decay disappears. For instance, when $a = b = 8$ (in such a waveguide ten modes at the transition frequency can propagate long distances along the axis: TE₁₀, TE₀₁, TE₂₀, TE₀₂, TE₁₁, TE₁₂, TE₂₁, TM₁₁, TM₁₂, TM₂₁), we observe that upon the spontaneous decay of any Zeeman sublevel m_J , other sublevels are almost not populated. Herewith, all the energy of initial excitation transfers to the electromagnetic field, and the decay dynamics can be described by a traditional single-exponential law with a good accuracy.

B. Diatomic effect

Alteration of the spatial structure of modes of the electromagnetic field in a waveguide leads not only to the modification of single-atom properties, but also qualitatively changes the character of any electromagnetic interaction between different atoms; in particular, the most pronounced dipole-dipole interaction. This effect also dramatically depends on the ratio between the transition frequency ω_0 and the cutoff frequency of a waveguide ω^c . In the case of $\omega_0 < \omega^c$, photon exchange between atoms is caused by near-field effects, so at long distances it is suppressed [47]. This situation is a lot like that taking place in a Fabry-Perot cavity with small separation between the mirrors, when single-atom spontaneous decay of some Zeeman sublevels is suppressed, but near-field energy exchange between different atoms recovers decay dynamics [41,42]. In the opposite case, $\omega_0 > \omega^c$, the dipole-dipole interaction is essentially long range, and the dynamics of a

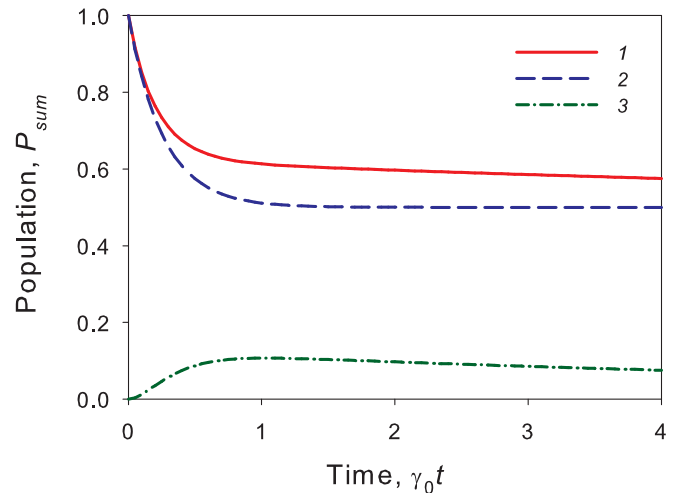


FIG. 3. Population of the excited state; $a = 4$, $b = 2$, $x_1 = x_2 = a/2$, $y_1 = y_2 = b/2$, $z_2 - z_1 = 107$. 1, first atom in the presence of second one; 2, first atom in the absence of second one; 3, second atom.

given atom can be significantly affected even by far-distant atoms [48].

Let us consider two atoms in a single-mode waveguide with transverse sizes $a = 4$, $b = 2$. The first atom is located at the point x_1, y_1, z_1 ; the second at x_2, y_2, z_2 . We assume that at initial time only one Zeeman sublevel $m_J = -1$ of the first atom is populated. The second atom is in the ground state.

Figure 3 shows the dynamics of the total excited state population $P_{\text{sum}}(t)$, calculated as a sum of $P_e(t)$ over all the Zeeman sublevels, separately for the first and for the second atom. In order to compare, we show the curve corresponding to the single-atom case, when the second atom is absent. Figure 3 demonstrates two main results. The first one is that the effect of incomplete spontaneous decay takes place in the diatomic problem. The total excited state population of the first atom in the presence of the second one asymptotically approaches to 0.5 at large times (we have checked it at any timescale). The second result is that a significant energy exchange between the atoms takes place even when the interatomic distance is very large. For the considered parameters, interatomic separation is 17 times greater than resonant wavelength. In free space, the dipole-dipole interaction at such distances is negligible. Herewith, in a waveguide, the population of the excited state of the second atom reaches 10%. Accordingly, one can see a significant difference in the dynamics of the first atom for the cases of the presence and absence of the second one.

We have studied the maximal population of the excited state of second atom $\max(P_{\text{sum},2})$ depending on the interatomic separation along the axis of a waveguide $\Delta z = z_2 - z_1$ (see Fig. 4). We have analyzed the case when both atoms are located at the axis of a waveguide, as well as when the first atom is at the axis and the second one at another position. Figure 4 demonstrates a periodical character of the long-range dipole-dipole interaction. In a single-mode waveguide that we considered, the spatial period is $k_0 T_s = \pi / \sqrt{1 - [\pi / (k_0 a)]^2}$; it is two times less than the spatial period of the TE₁₀ wave at the transition frequency. We noticed an interesting feature,

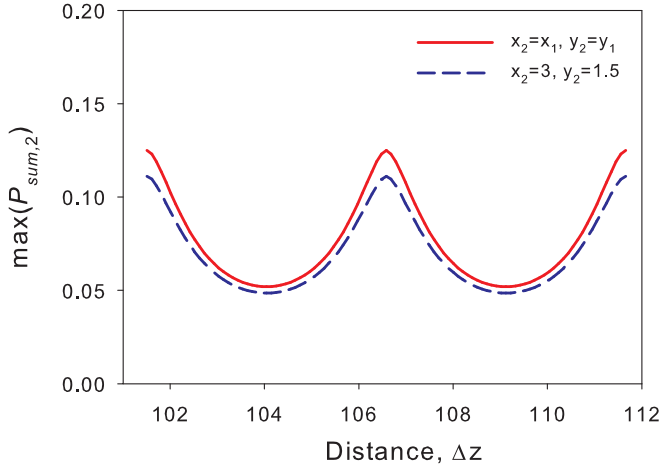


FIG. 4. Maximal population of the excited state of the second atom; $a = 4$, $b = 2$, $x_1 = a/2$, $y_1 = b/2$.

that the maximum of the dependence shown in Fig. 4 is, surprisingly, exactly $1/8$ for the case when both atoms are at the z axis and $1/9$ for the second considered case.

In the diatomic case, the Green's matrix has a size of 6×6 , so obtaining analytical expressions is much more complicated than in the case of a single atom. However, our analysis shows that in the specific case of far-distant atoms in a single-mode waveguide, the Green's matrix has only two nonzero eigenvalues:

$$\lambda_{1,2} = r_1 + r_3 \pm \sqrt{(r_1 - r_3)^2 + 4r_2^2}, \quad (11)$$

where $r_1 = -i\gamma'/4$, γ' is given by Eq. (10), $r_3 = -i\gamma''/4$, γ'' is determined by the same equation as γ' substituting x_2 instead of x_1 , and

$$r_2 = -\frac{3i\pi\gamma_0}{2k_0^2 ab \sqrt{1 - \left(\frac{\pi}{k_0 a}\right)^2}} \sin\left(\frac{\pi x_1}{a}\right) \sin\left(\frac{\pi x_2}{a}\right) \times \exp\left[i|z_2 - z_1| \sqrt{1 - \left(\frac{\pi}{k_0 a}\right)^2}\right]. \quad (12)$$

Both λ_1 and λ_2 are complex numbers, $\text{Im}(\lambda_{1,2}) < 0$. The dynamics of the quantum amplitudes of the onefold atomic excited states is given as follows:

$$b_{e_i, m_j}(t) = u_{i, m_j} + v_{i, m_j} \exp(-i\lambda_1 t) + w_{i, m_j} \exp(-i\lambda_2 t). \quad (13)$$

To obtain the coefficients u_{i, m_j} , v_{i, m_j} , and w_{i, m_j} , we need to solve the system of linear algebraic equations with full matrix 6×6 numerically.

IV. CONCLUSION

In conclusion, we considered the dynamics of atomic excitation prepared in a waveguide. We found out the effect of incomplete spontaneous decay—when the excited state population asymptotically approaches to a nonzero value at large times, under the conditions when the atomic transition frequency is larger than the cutoff frequency of a waveguide

and far from the vicinities of the cutoffs. The discovered effect is explained by polarization selection. It has been predicted in a single-mode waveguide with rectangular cross section both for the single-atom case and for the diatomic case when the long-range dipole-dipole interaction significantly affects the atomic dynamics.

ACKNOWLEDGMENTS

This work was supported by the Russian Science Foundation (Grant No. 17-12-01085). A.S.K. appreciates financial support from the Foundation for the Advancement of Theoretical Physics and Mathematics “BASIS” and Russian President Grant for Young Candidates of Sciences (project MK-1452.2020.2).

APPENDIX

As we assume an infinite length of a waveguide, the sum over the field variables in Eq. (9) should be calculated in the limit of infinite length of the quantization volume along the z axis, $L_q \rightarrow \infty$. This implies summation over the types of field modes in a waveguide (TE and TM), summation over the transverse indexes m and n , as well as the integration over continuous variable k_z :

$$\sum_g \text{ or } \sum_{ee} \rightarrow \frac{L_q}{2\pi} \sum_{\text{TE, TM}} \sum_{m, n} \int_{-\infty}^{+\infty} dk_z.$$

To simplify the calculations, it is convenient to perform summation by separate parts:

- (1) over TE modes with $n = 0$;
- (2) over TE modes with $m = 0$;
- (3) over TE modes with positive integer m and n ;
- (4) over TM modes (with positive integer m and n).

In accordance with this decomposition, we denote the part of the Green's matrix $G_{ee'}(\omega)$, which is calculated by the sum over the modes of the first group, as $G_{ee'}^I(\omega)$; second, $G_{ee'}^{II}(\omega)$; third, $G_{ee'}^{III}(\omega)$; and fourth, $G_{ee'}^{IV}(\omega)$. Applying the so-called polar approximation (i.e., neglecting retardation effects), one obtains the following expressions.

Sum over TE modes with $n = 0$

$$G_{ee'}^I(\omega_0)|_{i=j} = 8i\pi \frac{d_{e_j; s_j}^y d_{g_i; e_i}^y}{\gamma_0 ab} \times \sum_{m=1}^{\left[\frac{k_0 a}{\pi}\right]} \frac{k_0^2}{\sqrt{k_0^2 - k_m^2}} \sin^2(k_m x_i), \quad (A2)$$

$$G_{ee'}^I(\omega_0)|_{i \neq j} = 8\pi \frac{d_{e_j; s_j}^y d_{g_i; e_i}^y}{\gamma_0 ab} \times \left\{ i \sum_{m=1}^{\left[\frac{k_0 a}{\pi}\right]} \sin(k_m x_j) \sin(k_m x_i) \times \exp(i|z_j - z_i| \sqrt{k_0^2 - k_m^2}) \frac{k_0^2}{\sqrt{k_0^2 - k_m^2}} \right.$$

$$+ \sum_{m=\left[\left[\frac{k_0 a}{\pi}\right]\right]+1}^{+\infty} \sin(k_m x_j) \sin(k_m x_i) \times \exp(-|z_j - z_i| \sqrt{k_m^2 - k_0^2}) \frac{k_0^2}{\sqrt{k_m^2 - k_0^2}} \}. \quad (\text{A3})$$

Here the index i denotes quantities corresponding to the atom which transit from excited state to ground state, and the index j is related to the atom which performs reverse transition. Double brackets means the integer part, and i means imaginary unit.

Sum over TE modes with $m = 0$

$$G_{ee'}^{\text{II}}(\omega_0)|_{i=j} = 8i\pi \frac{d_{e_j;g_j}^x d_{g_i;e_i}^x}{\gamma_0 ab} \sum_{n=1}^{\left[\left[\frac{k_0 b}{\pi}\right]\right]} \frac{k_0^2}{\sqrt{k_0^2 - k_n^2}} \sin^2(k_n y_i), \quad (\text{A4})$$

$$G_{ee'}^{\text{II}}(\omega_0)|_{i \neq j} = 8\pi \frac{d_{e_j;g_j}^x d_{g_i;e_i}^x}{\gamma_0 ab} \left\{ i \sum_{n=1}^{\left[\left[\frac{k_0 b}{\pi}\right]\right]} \sin(k_n y_j) \sin(k_n y_i) \times \exp(i|z_j - z_i| \sqrt{k_0^2 - k_n^2}) \frac{k_0^2}{\sqrt{k_0^2 - k_n^2}} + \sum_{n=\left[\left[\frac{k_0 b}{\pi}\right]\right]+1}^{+\infty} \sin(k_n y_j) \sin(k_n y_i) \times \exp(-|z_j - z_i| \sqrt{k_n^2 - k_0^2}) \frac{k_0^2}{\sqrt{k_n^2 - k_0^2}} \right\}. \quad (\text{A5})$$

Sum over TE modes with positive integer m and n

$$G_{ee'}^{\text{III}}(\omega_0)|_{i=j} = \frac{16i\pi}{\gamma_0 ab} \times \sum_{m,n:\sqrt{k_m^2+k_n^2}<k_0} \frac{D_{mn}^{\text{III}}}{\sqrt{k_0^2 - k_m^2 - k_n^2}}, \quad (\text{A6})$$

$$G_{ee'}^{\text{III}}(\omega_0)|_{i \neq j} = \frac{16\pi}{\gamma_0 ab} \left\{ i \sum_{m,n:\sqrt{k_m^2+k_n^2}<k_0} \frac{D_{mn}^{\text{III}}}{\sqrt{k_0^2 - k_m^2 - k_n^2}} \times \exp(i|z_j - z_i| \sqrt{k_0^2 - k_m^2 - k_n^2}) + \sum_{m,n:\sqrt{k_m^2+k_n^2}>k_0} \frac{D_{mn}^{\text{III}}}{\sqrt{k_m^2 + k_n^2 - k_0^2}} \times \exp(-|z_j - z_i| \sqrt{k_m^2 + k_n^2 - k_0^2}) \right\}, \quad (\text{A7})$$

$$D_{mn}^{\text{III}} = \frac{k_0^2}{k_m^2 + k_n^2} [k_n d_{e_j;g_j}^x \cos(k_m x_j) \sin(k_n y_j) - k_m d_{e_j;g_j}^y \sin(k_m x_j) \cos(k_n y_j)] \times [k_n d_{g_i;e_i}^x \cos(k_m x_i) \sin(k_n y_i) - k_m d_{g_i;e_i}^y \sin(k_m x_i) \cos(k_n y_i)]. \quad (\text{A8})$$

Sum over TM modes (with positive integer m and n)

$$G_{ee'}^{\text{IV}}(\omega_0)|_{i=j} = \frac{16i\pi}{\gamma_0 ab} \times \sum_{m,n:\sqrt{k_m^2+k_n^2}<k_0} D_{mn}^{(\text{IV})1} \sqrt{k_0^2 - k_m^2 - k_n^2} + \frac{D_{mn}^{(\text{IV})3}}{\sqrt{k_0^2 - k_m^2 - k_n^2}}, \quad (\text{A9})$$

$$G_{ee'}^{\text{IV}}(\omega_0)|_{i \neq j} = -\frac{16\pi}{\gamma_0 ab} \left\{ (-i) \sum_{m,n:\sqrt{k_m^2+k_n^2}<k_0} \exp(i|z_j - z_i| \sqrt{k_0^2 - k_m^2 - k_n^2}) \times \left[D_{mn}^{(\text{IV})1} \sqrt{k_0^2 - k_m^2 - k_n^2} + i D_{mn}^{(\text{IV})2} \text{sgn}(z_j - z_i) + \frac{D_{mn}^{(\text{IV})3}}{\sqrt{k_0^2 - k_m^2 - k_n^2}} \right] + \sum_{m,n:\sqrt{k_m^2+k_n^2}>k_0} \exp(-|z_j - z_i| \sqrt{k_m^2 + k_n^2 - k_0^2}) \times \left[D_{mn}^{(\text{IV})1} \sqrt{k_m^2 + k_n^2 - k_0^2} + D_{mn}^{(\text{IV})2} \text{sgn}(z_j - z_i) - \frac{D_{mn}^{(\text{IV})3}}{\sqrt{k_m^2 + k_n^2 - k_0^2}} \right] \right\}, \quad (\text{A10})$$

$$D_{mn}^{(\text{IV})1} = \frac{1}{k_m^2 + k_n^2} [k_m d_{e_j;g_j}^x \cos(k_m x_j) \sin(k_n y_j) + k_n d_{e_j;g_j}^y \sin(k_m x_j) \cos(k_n y_j)] \times [k_m d_{g_i;e_i}^x \cos(k_m x_i) \sin(k_n y_i) + k_n d_{g_i;e_i}^y \sin(k_m x_i) \cos(k_n y_i)], \quad (\text{A11})$$

$$\begin{aligned}
D_{mn}^{(IV)2} = & d_{g_i;e_i}^z \sin(k_m x_i) \sin(k_n y_i) [k_m d_{e_j;g_j}^x \cos(k_m x_j) \sin(k_n y_j) \\
& + k_n d_{e_j;g_j}^y \sin(k_m x_j) \cos(k_n y_j)] - d_{e_j;g_j}^z \sin(k_m x_j) \sin(k_n y_j) \\
& \times [k_m d_{g_i;e_i}^x \cos(k_m x_i) \sin(k_n y_i) + k_n d_{g_i;e_i}^y \sin(k_m x_i) \cos(k_n y_i)], \tag{A12}
\end{aligned}$$

$$D_{mn}^{(IV)3} = d_{e_j;g_j}^z d_{g_i;e_i}^z (k_m^2 + k_n^2) \sin(k_m x_j) \sin(k_n y_j) \sin(k_m x_i) \sin(k_n y_i). \tag{A13}$$

-
- [1] E. M. Purcell, Spontaneous Emission Probabilities at Radio Frequencies, in *Proceedings of the American Physical Society* (American Physical Society, Cambridge, MA, 1946), Vol. 69, p. 681.
- [2] G. S. Agarwal, *Phys. Rev. A* **12**, 1475 (1975).
- [3] D. Kleppner, *Phys. Rev. Lett.* **47**, 233 (1981).
- [4] V. V. Klimov and M. Ducloy, *Phys. Rev. A* **62**, 043818 (2000).
- [5] V. V. Klimov and M. Ducloy, *Phys. Rev. A* **69**, 013812 (2004).
- [6] V. I. Yudson and P. Reincker, *Phys. Rev. A* **78**, 052713 (2008).
- [7] V. A. Pivovarov, A. S. Sheremet, L. V. Gerasimov, V. M. Porozova, N. V. Corzo, J. Laurat, and D. V. Kupriyanov, *Phys. Rev. A* **97**, 023827 (2018).
- [8] N. V. Corzo, B. Gouraud, A. Chandra, A. Goban, A. S. Sheremet, D. V. Kupriyanov, and J. Laurat, *Phys. Rev. Lett.* **117**, 133603 (2016).
- [9] V. P. Bykov, *Kvantovaya Elektron. 1*, 1557 (1974) [*Sov. J. Quantum Electron.* **4**, 861 (1975)].
- [10] P. Lambropoulos, G. M. Nikolopoulos, T. R. Nielsen, and S. Bay, *Rep. Prog. Phys.* **63**, 455 (2000).
- [11] D. Petrosyan and M. Fleischhauer, *Phys. Rev. Lett.* **100**, 170501 (2008).
- [12] P.-B. Li, Y. Gu, Q.-H. Gong, and G.-C. Guo, *Phys. Rev. A* **79**, 042339 (2009).
- [13] C.-H. Yan and L. F. Wei, *Phys. Rev. A* **94**, 053816 (2016).
- [14] N.-C. Kim, M.-C. Ko, and Q.-Q. Wang, *Plasmonics* **10**, 611 (2015).
- [15] J.-Q. Liao, J.-F. Huang, Y.-X. Liu, L.-M. Kuang, and C. P. Sun, *Phys. Rev. A* **80**, 014301 (2009).
- [16] L. Zhou, L.-P. Yang, Y. Li, and C. P. Sun, *Phys. Rev. Lett.* **111**, 103604 (2013).
- [17] L. Neumeier, M. Leib, and M. J. Hartmann, *Phys. Rev. Lett.* **111**, 063601 (2013).
- [18] D. E. Chang, A. S. Sorensen, E. A. Demler, and M. D. Lukin, *Nat. Phys.* **3**, 807 (2007).
- [19] O. Kyriienko and A. S. Sorensen, *Phys. Rev. Lett.* **117**, 140503 (2016).
- [20] Z. Liao, H. Nha, and M. S. Zubairy, *Phys. Rev. A* **93**, 033851 (2016).
- [21] M. Bradford, K. C. Obi, and J.-T. Shen, *Phys. Rev. Lett.* **108**, 103902 (2012).
- [22] I. Y. Eremchev, N. A. Lozing, A. A. Baev, A. O. Tarasevich, M. G. Gladush, A. A. Rozhentsov, and A. V. Naumov, *JETP Lett.* **108**, 30 (2018).
- [23] A. V. Naumov, A. A. Gorshelev, M. G. Gladush, T. A. Anikushina, A. V. Golovanova, J. Kohler, and L. Kador, *Nano Lett.* **18**, 6129 (2018).
- [24] O. Morice, Y. Castin, and J. Dalibard, *Phys. Rev. A* **51**, 3896 (1995).
- [25] J. D. Jackson, *Classical Electrodynamics* (Wiley, New York, 1962).
- [26] W. R. Raudorf, *Am. J. Phys.* **46**, 35 (1978).
- [27] I. M. Sokolov, D. V. Kupriyanov, and M. D. Havey, *J. Exp. Theor. Phys.* **112**, 246 (2011).
- [28] L. L. Foldy, *Phys. Rev.* **67**, 107 (1945).
- [29] M. J. Stephen, *J. Chem. Phys.* **40**, 669 (1964).
- [30] D. A. Hutchinson and H. F. Hamerka, *J. Chem. Phys.* **41**, 2006 (1964).
- [31] R. Bonifacio, P. Schwendimann, and F. Haake, *Phys. Rev. A* **4**, 302 (1971).
- [32] R. Bonifacio, P. Schwendimann, and F. Haake, *Phys. Rev. A* **4**, 854 (1971).
- [33] Z. Ficek, R. Tanas, and S. Kielich, *Opt. Acta* **33**, 1149 (1986).
- [34] Ya. A. Fofanov, A. S. Kuraptsev, I. M. Sokolov, and M. D. Havey, *Phys. Rev. A* **84**, 053811 (2011).
- [35] I. M. Sokolov, A. S. Kuraptsev, D. V. Kupriyanov, M. D. Havey, and S. Balik, *J. Mod. Opt.* **60**, 50 (2013).
- [36] A. S. Kuraptsev and I. M. Sokolov, *Phys. Rev. A* **91**, 053822 (2015).
- [37] S. Roof, K. Kemp, M. Havey, I. M. Sokolov, and D. V. Kupriyanov, *Opt. Lett.* **40**, 1137 (2015).
- [38] S. E. Skipetrov, I. M. Sokolov, and M. D. Havey, *Phys. Rev. A* **94**, 013825 (2016).
- [39] A. S. Kuraptsev and I. M. Sokolov, *Laser Phys.* **27**, 115201 (2017).
- [40] A. S. Kuraptsev, I. M. Sokolov, and M. D. Havey, *Phys. Rev. A* **96**, 023830 (2017).
- [41] A. S. Kuraptsev and I. M. Sokolov, *J. Exp. Theor. Phys.* **123**, 237 (2016).
- [42] A. S. Kuraptsev and I. M. Sokolov, *Phys. Rev. A* **94**, 022511 (2016).
- [43] A. S. Kuraptsev and I. M. Sokolov, *J. Exp. Theor. Phys.* **127**, 455 (2018).
- [44] A. S. Kuraptsev and I. M. Sokolov, *Laser Phys.* **28**, 085203 (2018).
- [45] A. S. Kuraptsev and I. M. Sokolov, *Phys. Rev. A* **100**, 063836 (2019).
- [46] P. Longo, P. Schmitteckert, and K. Busch, *Phys. Rev. A* **83**, 063828 (2011).
- [47] G. Fiscelli, L. Rizzuto, and R. Passante, *Phys. Rev. A* **98**, 013849 (2018).
- [48] Y. Jiang, *J. Phys. Commun.* **2**, 055002 (2018).